Cardiac Apoptosis in Severe Relapsing Fever Borreliosis

Diana Londoño,[1] Yunhong Bai,[1] Wolfram R. Zückert,[2] Harald Gelderblom,[1]
and Diego Cadavid[1]*

*Department of Neurology and Neuroscience and Center for the Study of Emerging Pathogens, University of Medicine
and Dentistry of New Jersey-New Jersey Medical School, Newark, New Jersey,[1] and Department of
Microbiology, Molecular Genetics and Immunology, The University of Kansas
Medical Center, Kansas City, Kansas[2]*

Previous studies revealed that the heart suffers significant injury during experimental Lyme and relapsing fever borreliosis when the immune response is impaired (D. Cadavid, Y. Bai, E. Hodzic, K. Narayan, S. W. Barthold, and A. R. Pachner, Lab. Investig. 84:1439–1450, 2004; D. Cadavid, T. O'Neill, H. Schaefer, and A. R. Pachner, Lab. Investig. 80:1043–1054, 2000; and D. Cadavid, D. D. Thomas, R. Crawley, and A. G. Barbour, J. Exp. Med. 179:631–642, 1994). To investigate cardiac injury in borrelia carditis, we used antibody-deficient mice persistently infected with isogenic serotypes of the relapsing fever agent *Borrelia turicatae*. We studied infection in hearts 1 to 2 months after inoculation by TaqMan reverse transcription-PCR and immunohisto-chemistry (IHC) and inflammation by hematoxylin and eosin and trichrome staining, IHC, and in situ hybridization (ISH). We studied apoptosis by terminal transferase-mediated DNA nick end labeling assay and measured expression of apoptotic molecules by RNase protection assay, immunofluorescence, and immunoblot. All antibody-deficient mice, but none of the immunocompetent controls, developed persistent infection of the heart. Antibody-deficient mice infected with serotype 2 had more severe cardiac infection and injury than serotype 1-infected mice. The injury was more severe around the base of the heart and pericardium, corresponding to sites of marked infiltration by activated macrophages and upregulation of interleukin-6 (IL-6). Infected hearts showed evidence of apoptosis of macrophages and cardiomyocytes as well as significant upregulation of caspases, most notably caspase-1. We conclude that persistent infection with relapsing fever borrelias causes significant loss of cardiomyocytes associated with prominent infiltration by activated macrophages, upregulation of IL-6, induction of caspase-1, and apoptosis.

Multiple infectious agents have been associated with carditis (45). The most commonly identified agents are viruses, notably coxsackie B, but several bacteria, protozoa, and fungi can also cause carditis (28, 37, 41). Spirochetes are one group of bacteria with a predilection for cardiac infection. Syphilis, caused by the spirochete *Treponema pallidum*, was a major cause of cardiovascular disease prior to the discovery of penicillin (35). Lyme borreliosis, another multisystemic infection caused by the spirochete *Borrelia burgdorferi*, is now the most common vector-borne disease in the United States (43). Of the several thousand cases in the United States each year, up to 10% develop cardiac complications (5). The prevalence of asymptomatic carditis can be as high as 30% (56). Atrioventricular block is the most serious acute manifestation (55, 56), but myocarditis and heart failure also occur (23, 24). The overall prognosis in most cases is good, although delayed recovery can occur (9). The pathogenesis of borrelia carditis is incompletely understood. Only rarely have human tissues from Lyme carditis or the organism isolated from human heart been examined (52). Microscopy has shown lymphoplasmacytic infiltrate in the myocardium with macrophages and necrotic cardiomyocytes (54).

In previous studies we found severe carditis in nonhuman primates persistently infected with the Lyme disease spirochete *Borrelia burgdorferi* (11, 13) and in antibody-deficient mice (*scid*) persistently infected with the relapsing fever spirochete *Borrelia turicatae* (16). Relapsing fever spirochetes are best known for their ability to evade the host's immune response by sequential expression of surface lipoproteins known as variable major proteins, which come in two molecular sizes: variable small proteins (Vsp) and variable large proteins (Vlp) (25). Using antibody-deficient mice, we have identified two isogenic serotypes of *B. turicatae* which differ only in their Vsp but show marked differences in their virulence and tissue tropism: serotype 2 is defined by expression of a 20-kDa Vsp2, which is more virulent than serotype 1, which is defined by a 23-kDa Vsp1 (14, 16). We used mice inoculated with serotype 1 or serotype 2 to investigate the mechanism of cardiac injury in systemic borreliosis. We found that antibody deficiency results in persistent infection with significant loss of cardiomyocytes and documented prominent apoptotic changes in injured hearts.

MATERIALS AND METHODS

Strains and culture conditions. Serotypes 1 and 2 of *Borrelia turicatae* have been previously described (16, 15, 46). Borrelias were cultured in Barbour-Stoenner-Kelly II (BSK-II) medium with 12% rabbit serum and counted in a Petroff-Hauser chamber under phase-contrast microscopy (7). The purity of the populations was assessed before infection by using Western blotting with serotype-specific monoclonal antibodies (15, 46).

Animal infections. Four- to 6-week-old female mice were inoculated intraperitoneally with 10^3 cells of serotype 1 or 2 of *B. turicatae* in 200 µl of phosphate-buffered saline (PBS) or PBS alone as a control. Antibody-deficient mice were *scid* (severe combined immunodeficiency) (Charles Rivers), Igh6 deficient

* Corresponding author. Mailing address: Department of Neurology and Neuroscience and Center for the Study of Emerging Pathogens, UMDNJ-New Jersey Medical School, 185 South Orange Avenue, MSB H506, Newark, NJ 07103. Phone: (973) 972-8686. Fax: (973) 972-5059. E-mail: cadavidi@umdnj.edu.

(Igh6$^{-/-}$), or Rag1 deficient (Rag1$^{-/-}$) (Jax mice). Immunocompetent mice of the C3H/HeJ and SWR/J genetic backgrounds and outbred Swiss Webster mice (purchased from Taconic or Harlan) as well as Toll-like receptor 2 (TLR2)-deficient mice in the C57BL/6 background (bred in house) were similarly inoculated for comparison with the antibody-deficient mice. The housing and care of the mice were in accordance with the Animal Welfare Act and Federal guidelines in facilities accredited by the American Association for Accreditation of Laboratory Animal Care. Antibody-deficient mice were maintained in a germ-free environment before and after infection.

Tissue and fluid collection. Mice were anesthetized with isoflurane prior to euthanasia by exanguination with cardiac puncture. Total body perfusion with 30 ml of PBS was performed prior to necropsy. For borrelia cultures, whole hearts were removed and rinsed three times with 1 ml of sterile PBS in 2-ml microcentrifuge tubes followed by brief homogenization in BSK-II media using lysing matrix D (Bio101). Blood and heart homogenates were centrifuged for 5 s at 7,000 × g prior to inoculation of the supernatant into BSK-II culture tubes. All cultures were examined for spirochetes for 2 weeks.

Histology. The hearts were removed at necropsy and were fixed in 4% paraformaldehyde for 48 h at 4°C, followed by embedding in paraffin or cryopreserved in 20% sucrose. The samples were then frozen in dry ice-cold isopentane and embedded in cryomatrix (Shandon). Paraffin-embedded tissue blocks were sectioned at 5 μm and frozen blocks at 10 μm. Hematoxylin and eosin (H&E) and Masson's trichrome stains were prepared by standard technique. All tissue sections were examined with standard light or fluorescence microscopy masked to the infectious status. Inflammation was defined by the characteristic morphology of mononuclear inflammatory cells on H&E staining. Digital image analysis was used to measure the loss of the red color of Masson's trichrome staining by cardiomyocytes as evidence of cell loss and/or injury.

Immunohistochemistry. Immunohistochemistry was performed essentially as described previously (14). The primary antibodies were rabbit polyclonal anti-Bax (Santa Cruz 493-R) at 1 μg/ml or mouse monoclonal antibody anti-Vsp1 or anti-Vsp2 diluted 1:1,000 (15, 46). The secondary reagents were anti-rabbit or anti-mouse biotinylated antibodies (Biogenex), and the tertiary reagent was streptavidin-labeled horseradish peroxidase (Biogenex). Incubation time was 30 min for the primary and 20 min for the secondary and tertiary reagents. The chromogen was 3,3-diaminobenzidine tetrahydrochloride (DAB) in 0.24% H_2O_2 for 5 to 15 min. The counterstaining was Mayer's hematoxylin diluted 1/5 in H_2O for 1 min. Affinity-purified rat and rabbit immunoglobulin G (IgG) (Sigma) at 1 to 2 μg/ml were used as negative controls.

Immunofluorescence. Ten-micron frozen sagital heart sections from infected ($n = 2$) or uninfected ($n = 2$) Igh6-deficient mice were mounted on superfrost glass slides (Fisher), blocked with a casein solution (Biogenex) (14), and stained with rat monoclonal antibody anti-mouse caspase-1 or -11 (hybridomas) diluted 1/10 (a kind gift from J. Yuan, Harvard Medical School) (27) and/or 1 μg/ml of rat anti-mouse F4/80 (Serotec MCAP497). The caspase antibodies were incubated overnight and the F4/80 for 30 min. The secondary reagents were fluorescein isothiocyanate (FITC)- or tetramethyl rhodamine isocyanate (TRITC)-labeled anti-rat monoclonal antibodies (Sigma) diluted 1/300. Images were obtained with an Olympus BX40 microscope with an Optronics digital camera using FITC, TRITC, and dual FITC/TRITC filters.

TUNEL. Apoptosis was studied using the terminal transferase-mediated DNA nick end labeling (TUNEL) assay. Deparaffinized heart sections were digested with proteinase K (20 μg/ml; Worthington) for 30 min to expose the DNA, endogenous peroxidase activity was reduced by incubation with 3% H_2O_2 for 10 min at room temperature, and DNA fragments were labeled with biotinylated conjugated dUTP using TdT (Roche Molecular Biochemicals) for 1 h at 37°C and visualized with horseradish peroxidase-labeled streptavidin with DAB as the chromogen. The assay was standardized using sections treated with DNase I as a positive control. Negative control sections were incubated without the TdT enzyme.

In situ hybridization. The oligonucleotide primers used for interleukin-6 (IL-6) reverse transcription-PCR (RT-PCR) were 5′-ATGAACTCCTTCTCC ACAAG3′ and 5′-CGGAATTCTACATTTGCCGAAGAGCCCTCAG-3′, corresponding to positions 1 to 20 and 616 to 639 on the *Macaca mulatta* IL-6 cDNA (GenBank accession no. L26028). This riboprobe, although designed for use in tissues from nonhuman primates, was found to be cross-reactive with human and mouse tissues. PCR amplification was performed with *Taq* gold polymerase for 40 cycles at 94°C for 2 min, 60°C for 30 s, and 72°C for 30 s. PCR products were directly inserted into a pCR2.1 vector (Invitrogen, Carlsbad, CA). Plasmids were isolated and analyzed by restriction mapping and DNA sequencing. Digoxigenin-11-UTP single-stranded RNA probes (sense and antisense) were synthesized in vitro by transcription of linearized plasmid DNA templates. Digoxigenin RNA labeling (Sp6/T7) and detection kits from Roche were used. Nitroblue tetrazo-

lium–5-bromo-4-chloro-3-indolylphosphate was used for color detection. Quantification and efficiency of probe labeling were analyzed by serial dilution of test strips. Probes were used at a concentration of 2 μg/ml. The IL-6 sense and antisense probes had a length of 639 bp. Paraffin-embedded formalin-fixed heart sections were dewaxed in xylene and rehydrated in ascending alcohols. Sections were permeabilized for 30 min at 37°C in TE buffer (100 mM Tris-HCl, 50 mM EDTA, pH 8.0) containing 20 μg/ml RNase-free proteinase K. The slides were postfixed in diethyl pyrocarbonate-treated PBS containing 4% paraformaldehyde for 5 min at 4°C and incubated at 37°C for 1 h with prehybridization buffer (50% formamide, 5× SSC [1× SSC is 0.15 M NaCl plus 0.015 M sodium citrate], 5× Denhardt's solution, 100 mg/ml salmon sperm DNA, 0.25 mg/ml yeast tRNA). This was followed by incubation with 50 ml of hybridization buffer containing 2 μg/ml of digoxigenin-labeled RNA probe at 50°C overnight in a humid chamber. After incubation, the slides were washed with buffer 1 (100 mM Tris-HCl [pH 7.5], 150 mM NaCl) twice for 10 min, covered for 30 min with buffer 2 (1% blocking reagent), and incubated for 2 h in a humid chamber with anti-digoxigenin alkaline phosphatase-conjugated antibody diluted 1:500 (15 mU/ml) in buffer 2. This was followed by incubation for 10 min with buffer 3 (100 mM Tris-HCl [pH 9.5], 100 mM NaCl, 50 mM $MgCl_2$). Finally, the slides were covered with 200 μl color solution (4,840 μl of buffer 3, 125 μl of nitroblue tetrazolium, and 32.5 μl of 5-bromo-4-chloro-3-indolylphosphate) and incubated in a humid chamber for 2 to 24 h in the dark. After optimal color development, the reaction was stopped with buffer 4 (10 mM Tris-HCl [pH 8.0], 1 mM EDTA).

TaqMan RT-PCR. Borrelia in heart tissue was measured by TaqMan RT-PCR amplification of 16S rRNA using primers and probes common to the genus *Borrelia* essentially as described previously (6, 11). Total RNA was extracted with TRIzole reagent (Life Technologies). One microgram total RNA was used as template for RT. For quantification of the spirochetal load, cultured borrelias were counted in a Petroff-Hausser chamber by phase-contrast microscopy, and total RNA was extracted from known numbers of borrelias used in log_{10} dilutions to create a standard curve. PCRs with H_2O instead of cDNA were included as negative controls. The mouse housekeeping gene 18S rRNA was measured to control for the amount of input RNA using a kit from Applied Biosystems (4319413E).

For *vsp* RT-PCR, total RNA was extracted from heart with TRIzole reagent (Life Technologies), and 150 μg of total RNA was used as template for reverse transcription (RT) using reverse primer *Bt-vsp1R* (5′-TTAACAAMGTATCWA TTGCTGTATT-3′, corresponding to base pairs 1981 to 1957 of GenBank accession no. AF129434) (15). PCR amplification was carried out in a 25-μl reaction mixture containing 25 μl of forward primer *S34vspAB* (corresponding to base pairs GGAATTCCATATGTCTGAGGGCACTGTT of AF129434) and reverse primer *Bt-vsp1R*, giving a predicted PCR fragment size of 616 bp. There was an initial denaturation at 94°C for 1 min followed by 40 cycles of denaturation at 94°C for 50 s, annealing at 45°C for 30 s, and amplification at 60°C for 45 s, followed by a final extension at 60°C for 7 min.

RNA protection assay. ^{32}P-labeled riboprobes were incubated with 10 μg of total RNA and then subjected to RNase digestion using a kit from BD Pharmingen (Franklin Lakes, NJ) following the manufacturer's instructions. We used the mouse apoptosis multiprobe template set mAPO-1, which measures caspases 1, 2, 3, 6, 7, 8, 11, 12, and 14, and housekeeping genes L32 and GAPDH. Following electrophoresis on a 6% polyacrylamide gel, radiolabeled bands were visualized with a PhosphorImager (Amersham Biosciences). The optical density of the protected bands was measured with Image Quant Software (Molecular Dynamics), which was then normalized by the value of GAPDH in the same lane. Two separate RNase protection assays on different groups of mice were performed for consistency.

Immunoblot. Immunoblot for detection of caspase-1 and α-actinin were performed using 12% acrylamide with the minigel system (Bio-Rad) (15). The hearts were homogenized in the presence of protease inhibitors using lysine matrix D (Bio101 systems) as described before (6). Protein concentration was determined using the bicinchoninic acid protein assay (Pierce). The primary antibodies were rabbit polyclonal antibody anti-mouse caspase-1 p10 (Santa Cruz No. 514) at 1 μg/ml and mouse monoclonal anti-α-sarcomeric actinin (Sigma A7811) diluted 1/2,500. The secondary antibody was alkaline phosphatase-conjugated goat anti-rabbit or goat anti-mouse diluted 1/30,000. After incubation in fluorescence substrate ECF (Amersham RPN5785) for 5 min, the membranes were scanned with a Typhoon 8600 (Amersham Pharmacia Biotech Inc). Results were analyzed by densitometry using Image Quant Software, expressed as means (95% confidence interval), and compared with the amount of the mouse structural protein α-actinin to control for the amount of input protein.

Statistical analysis. Results are given as means (95% confidence interval of the means). Student's t test or nonparametric tests (Mann-Whitney test) were used to determine whether the differences between means were significant. The
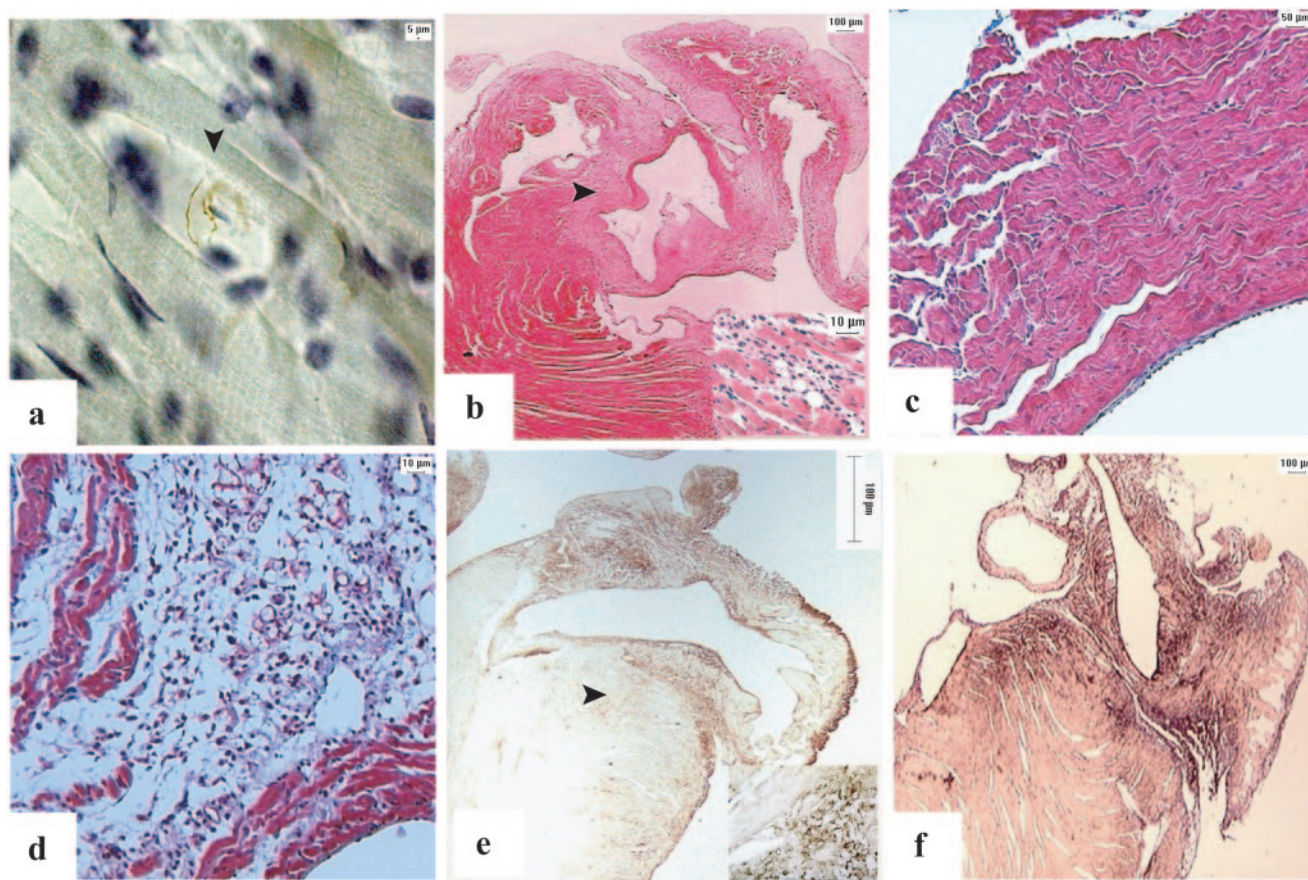
FIG. 1. Cardiac infection, inflammation, and loss of cardiomyocytes in relapsing fever borreliosis. a) Localization of *B. turicatae* serotype 2 (arrow) next to cardiomyocytes by immunohistochemistry. 400× magnification. b) A sagital H&E-stained heart section from a *scid* mouse persistently infected with *B. turicatae* shows inflammation (arrow) mainly at the base of the heart and the great vessels. 20× magnification. An adjacent 400× magnification field shows the inflammation in more detail. c) Masson's trichrome staining in PBS-inoculated mice shows intact cardiomyocytes in the atrium. 400× magnification. d) Masson's trichrome staining shows loss of cardiomyocytes in *B. turicatae* serotype 2-infected heart atrium (loss of red stain). 400× magnification. e) Immunohistochemistry for the macrophage activation marker F4/80 in a sagital heart section from a *scid* mouse persistently infected with *B. turicatae* shows prominent staining (brown color) at the base and periphery of the heart. 20× magnification. The adjacent picture shows activated macrophages at higher magnification (400× magnification). f) Presence of IL-6 mRNA by nonisotopic in situ hybridization (purple color) in a sagital heart section from a *scid* mouse persistently infected with *B. turicatae* serotype 2. 20× magnification.

chi-square test was used to compare differences in percentages. A *P* value of less than 0.05 was considered significant.

RESULTS

Infection. Phase-contrast microscopic examination of necropsy blood 1 to 2 months after inoculation revealed spirochetemia in all antibody-deficient mice (24 *scid*, 24 Igh6$^{-/-}$, and 16 Rag1$^{-/-}$) compared to none of the 22 immunocompetent (10 C3H/HeJ, 4 SWR/J, and 8 Swiss Webster) or 14 TLR2$^{-/-}$ mice. Heart cultures in BSK-II media revealed that antibody-deficient mice were significantly more susceptible to persistent cardiac infection than immunocompetent or TLR2$^{-/-}$ mice: 8 out of 12 heart cultures from *scid* mice inoculated with serotype 1 (4 out of 6) or 2 (4 out of 6) grew spirochetes compared to 0 out of 26 immunocompetent or TLR2$^{-/-}$ mice inoculated with serotype 1 ($P < 0.01$). All Igh6$^{-/-}$ and Rag1$^{-/-}$ mice also had persistent infection of the heart (H. Gelderbrom and D. Cadavid, unpublished data). None of the mice sham inoculated with PBS showed any evidence of spirochetemia or cardiac infection. Hearts from *scid* mice inoculated with serotype 1 or 2 or PBS as a control were immunostained with antibody to Vsp1 or Vsp2. Light microscopic examination showed abundant spirochetes expressing Vsp1 or Vsp2 in the base and periphery of the heart and in the extracellular matrix between cardiac fibers (Fig. 1a) as well as around the aorta and great vessels in all infected mice, but they were not seen in any of the uninfected controls. Expression of Vsp1 and Vsp2 in the heart of infected mice was confirmed by RT-PCR amplification of their expressed *vsp* genes (15 and data not shown). To investigate whether there were differences in the ability of serotypes 1 and 2 to infect the heart, we measured the spirochetal load per microgram of total heart RNA using TaqMan RT-PCR. For this, total RNA was extracted from whole hearts and measured by TaqMan RT-PCR with primers and probe for the *Borrelia* spp. 16S rRNA. The results showed there were five times more spirochetes in the heart from *scid* mice infected with serotype 2 than from those infected with serotype 1

TABLE 1. Spirochetal load and loss of cardiomyocytes in *scid* mice infected for 2 months with serotype 1 or 2 of *Borrelia turicatae* or PBS as a control

Infection	Spirochetal load[a]	Negative red staining in[b]:	
		Atrium	Ventricle
Serotype 1	10.7 (8.1–13.3)[c]	8.8[d]	2.4
Serotype 2	46.7 (30–63.6)	16.2	2.4
PBS	0	3.7	1.4

[a] Mean (standard deviations) of spirochetes per nanogram of cDNA of mouse 18S rRNA measured by TaqMan RT-PCR.

[b] Sum area in square micrometers (10^6) per $40\times$ microscopic sagital heart field not stained red with Masson's trichrome (Fig. 1c and d).

[c] $P < 0.001$ for the difference between serotypes 1 and 2 (Student's *t* test).

[d] $P < 0.05$, $P < 0.01$, and $P = 0.02$ for the differences in the heart base between serotype 1 and PBS, serotype 2 and PBS, and serotypes 1 and 2, respectively (Student's *t* test).

TABLE 2. Mean sum area positive for the activated macrophage marker F4/80 per $40\times$ microscopic field by immunohistochemistry (IHC) and for IL-6 mRNA by in situ hybridization (ISH) in heart sections from *scid* mice infected with serotype 1 or 2 of *Borrelia turicatae* or PBS as a control

Infection	F4/80 IHC area (μm^2, 10^5)		IL-6 ISH area (μm^2, 10^5)	
	Base	Ventricle	Base	Ventricle
Serotype 1	8.9[a]	3.4	11.2[b]	1.5
Serotype 2	11.5	3.4	13	1.5
PBS	0.4	0.3	0.8	0.2

[a] $P < 0.01$ for the difference in F4/80 immunostaining at the heart between serotype 1 or 2 and PBS; the difference between serotypes 1 and 2 was not statistically significant (Student's *t* test).

[b] $P < 0.01$ for the difference in IL-6 mRNA between serotype 1 or 2 and PBS (Student's *t* test). The difference between serotypes 1 and 2 was not statistically significant. The corresponding numbers for the IL-6 sense RNA probes were 0.001 for serotypes 1 and 2 and 0 for PBS.

(Table 1). The experiment was repeated, controlling for the amount of mouse housekeeping gene 18S rRNA and obtaining similar results (data not shown).

Cardiac inflammation. Microscopic examination of H&E-stained heart sections from all the antibody-deficient mice examined independent of their genotype (*scid*, Igh6$^{-/-}$, or Rag1$^{-/-}$) showed severe inflammation and injury (Fig. 1b to f). The inflammatory infiltrate was predominantly mononuclear and localized around the base of the heart, the pericardium, and between myocardial fibers. It was greatest in the atria and around the base of great vessels (Fig. 1b). Multifocal areas of cardiac fiber degeneration were seen throughout the heart but were more prominent in the atrium and periphery of the ventricles next to inflammatory infiltrates (inset in Fig. 1b). Immunostaining revealed that the majority of the inflammatory cells were activated macrophages (Fig. 1e). Only a few T cells were observed in Igh6$^{-/-}$ and none in *scid* or Rag1$^{-/-}$ mice, which are both B and T cell deficient (data not shown). In situ hybridization revealed that the area positive for activated macrophages was also strongly positive for interleukin-6 mRNA, a well-known inflammatory cytokine induced by borrelia lipoproteins (Fig. 1f) (49). Digital image analysis revealed that the extent of infiltration by activated macrophages and upregulation of IL-6 was similar in *scid* mice infected with either serotype (Table 2) but significantly increased compared to uninfected controls. None of the uninfected controls or immunocompetent mice examined microscopically showed any evidence of cardiac inflammation.

Loss of cardiomyocytes. We took advantage of the strong red color of Masson's trichrome stains on the cytoplasm of cardiomyocytes to measure their loss as a result of persistent infection in *scid* mice (Fig. 1c and d). Digital image analysis revealed the loss of 5 to 12 million and 1 million square microns of cardiomyocyte cytoplasm from the atrium and ventricle, respectively, per $40\times$ sagital heart section, as a result of the infection (Table 1) ($P < 0.01$ in infected versus uninfected samples for both the ventricle and the atrium). The loss of cardiomyocytes from the atrium was significantly higher with serotype 2 than with serotype 1 ($P = 0.02$).

Cardiac apoptosis. Examination of the injured areas in infected hearts on H&E staining revealed frequent fragmented nuclei, nuclear chromatin condensation, and dark staining of the cytoplasm, all an indication that apoptotic cell death was

taking place. To further investigate this we examined heart sections from infected and uninfected *scid* mice with the terminal deoxynucleotidyltransferase-mediated dUTP nick-end labeling (TUNEL) assay. We observed frequent TUNEL staining in both infiltrating inflammatory cells and also in cardiomyocytes from infected *scid* and Igh6$^{-/-}$ mice (Fig. 2a) but not in uninfected controls. The TUNEL of cardiomyocytes was more evident and distinct in areas with, or in close proximity to, inflammatory infiltrates. Positive control slides (DNA nicking induced by DNase I) had positive TUNEL staining in all nuclei (data not shown). The negative control sections stained with the TUNEL assay without TdT did not show any signal. Immunostaining for Bax, an inducer of apoptosis (42), provided further evidence that apoptotic cell death was taking place, as immune cells and cardiomyocytes from infected *scid* mice showed positive staining (Fig. 2b). These results revealed that persistent infection with *B. turicatae* caused apoptosis of cardiomyocytes. To investigate whether this also occurred in Lyme borreliosis, we did TUNEL assay in heart sections from rhesus macaques persistently infected with *Borrelia burgdorferi*. Previous studies had shown that persistent *B. burgdorferi* infection causes significant injury to the nonhuman primate heart (11, 13). The results showed frequent TUNEL staining in the nuclei of cardiomyocytes from infected rhesus macaques (Fig. 2c) but not in uninfected controls (data not shown). Microscopic examination of 10 consecutive $200\times$ TUNEL-stained fields from *scid* mice infected with *B. turicatae* showed 7 apoptotic cardiomyocytes in the atrium and 2 in the base; the corresponding numbers for the atrium and the ventricle from immunosuppressed rhesus macaques infected with *B. burgdorferi* were 16 and 4. This is, to our knowledge, the first report in vivo that persistent spirochetal infection causes apoptosis of cardiomyocytes. It also confirmed that cardiomyocytes are more affected in the atrium than in the ventricles.

During apoptosis, cell death is mediated by several caspases, a class of proteases of which more than 10 have been identified. To investigate whether caspases were upregulated in infected hearts, we did RNase protection assays. For this we measured the levels of caspase mRNA in infected ($n = 4$) and uninfected ($n = 4$) *scid* hearts necropsied 1 month after inoculation. The density of each caspase was adjusted to the density
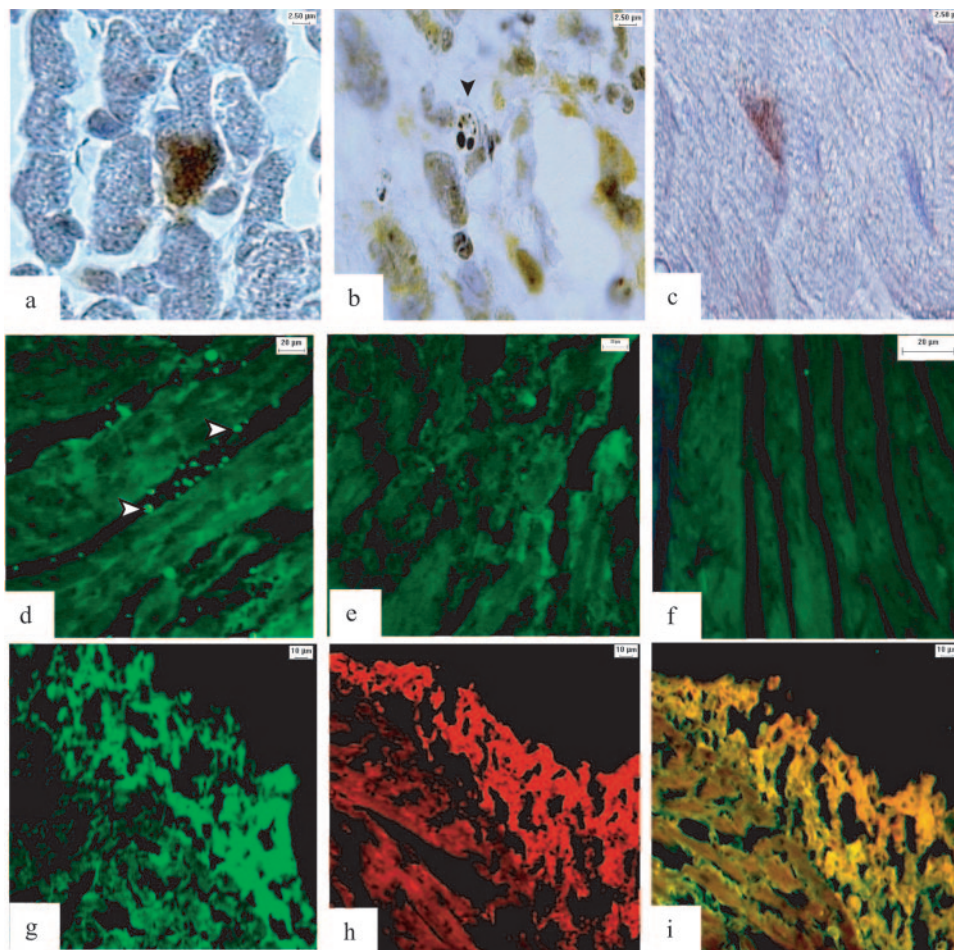
FIG. 2. Cardiac apoptosis in relapsing fever and Lyme borreliosis. a) Cardiomyocyte with positive TUNEL staining in the nucleus (brown color) of one Igh6$^{-/-}$ mouse persistently infected with *B. turicatae* serotype 2. Magnification, 1,000×. b) Apoptotic body (arrow) and expression of Bax (yellow color) in the heart of a *scid* mouse infected with *B. turicatae*. 1,000× magnification. c) TUNEL staining in the nucleus of a cardiomyocyte from an immunosuppressed nonhuman primate persistently infected with *B. burgdorferi*. 1,000× magnification. d) Anti-caspase-1 antibody shows green fluorescence in mononuclear cells from an Igh6$^{-/-}$ mouse infected with *B. turicatae* serotype 2. 400× magnification. e) Negative control section shows lack of staining in an area of severe inflammation and cardiac fiber degradation incubated with 2 μg/ml of rat IgG as a negative control. 400× magnification. f) Myocardium from an uninfected Igh6$^{-/-}$ mouse stained with anti-caspase-1 antibody shows no signal. 400× magnification. g) Periphery of the left ventricle near the atrium from an Igh6$^{-/-}$ mouse infected with serotype 1 and FITC stained with anticaspase-1 antibody (200× magnification). h) Consecutive section from the same mouse shows red fluorescence staining (TRITC) after incubation with anti-F4/80 antibody, a marker of activated macrophages. i) Double immunofluorescence staining with anti-caspase-1 (FITC) and anti-F4/80 (TRITC) antibodies shows yellow color, indicating colocalization, in the pericardium and membranes from nearby cardiomyocytes.

of the housekeeping gene GAPDH, and the results are expressed as ratios. The experiment was repeated a second time using new groups of *scid* mice for consistency. The results showed significant upregulation of several caspases in infected mice, most notably caspase-1 (Table 3). To confirm whether caspase-1 was upregulated at the protein level and their cell of origin, we did immunofluorescence. The results showed intense caspase-1 staining in mononuclear cells in infected (Fig. 2d) but not uninfected or control hearts (Fig. 2e and f). Double immunostaining revealed that activated macrophages (F4/80-positive cells) were the main source of caspase-1 (Fig. 2g to i). Extensive double-stained areas were observed in the periphery and base of the heart and next to areas of cardiomyocyte injury (Fig. 2i). Immunofluorescent staining with an antibody to caspase-3 showed some positive signal but much less than that with caspase-1 (data not shown). Probing

of whole-heart protein extracts from Igh6$^{-/-}$ mice with a different anti-mouse caspase-1 antibody (Santa Cruz) confirmed increased caspase-1 in infected hearts: densitometry of the caspase-1 band compared with the α-actinin-control band showed significantly higher expression of caspase-1 in infected mice compared to uninfected controls (Table 4). These results provided further evidence that persistent infection with *B. turicatae* causes upregulation of caspase-1 in the heart.

DISCUSSION

This study revealed that, compared to immunocompetent mice that are resistant to relapsing fever carditis, antibody-deficient mice develop persistent cardiac infection with severe inflammation and loss of cardiomyocytes. The finding that *scid*, Igh6$^{-/-}$, and Rag1$^{-/-}$ mice developed severe carditis is evi-

TABLE 3. Mean density ratio of various caspases to GAPDH by RNase protection assay in the heart of *scid* mice persistently infected with *B. turicatae* serotype 2 compared to uninfected controls (PBS)

Caspase	Serotype 2	PBS	P
1	26 (18–35)[a]	6 (5–6)	0.003
2	20 (11–30)	8 (6–10)	0.04
3	18 (10–26)	6 (5–6)	0.024
6	20 (11–29)	9 (8–10)	0.04
7	22 (14–31)	10 (6–13)	0.03
8	19 (12–26)	9 (7–10)	0.024
11	18 (11–24)	5 (4–6)	0.01
12	16 (9–22)	8 (7–8)	0.06

[a] Four to five mice per group were inoculated intraperitoneally with 10^3 cells of *B. turicatae* serotype 2 or PBS as a control, and their hearts were removed at necropsy 2 months later. Total RNA was subjected to RNase protection assay with ^{32}P-labeled riboprobes for mouse caspases or GAPDH and resolved by acrylamide electrophoresis. Results are expressed as the mean (95% confidence interval) density for each caspase band, multiplied by 100 and divided by the density of the respective GAPDH band.

TABLE 4. α-Actinin and caspase-1 protein levels by quantitative immunoblot in the heart of *scid* mice persistently infected with *B. turicatae* serotype 1 compared to uninfected controls (PBS)

Protein	Serotype 1	PBS
α-Actinin	2.31 (2.25–2.40)[a]	2.33 (2.05–2.60)
Caspase-1	1.75 (1.42–2.08)[b]	1.12 (1.01–1.23)

[a] Densitometry shows 1.5 times higher expression of caspase-1 in the heart from Igh6$^{-/-}$ mice ($n = 2$) persistently infected with serotype 1 of *B. turicatae* compared with uninfected controls ($n = 2$). Both groups showed similar expression of α-actinin. Results are expressed as the mean (95% confidence interval) arbitrary density units per 0.01 μg of protein extract (10^7).
[b] $P = 0.02$ for the difference in caspase-1 in the heart between serotype 1 and PBS; the difference between α-actininin in serotype 1 and PBS groups was not statistically significant (Student's *t* test).

dence that the increased susceptibility to relapsing fever borreliosis is due to B-cell deficiency. This is consistent with the finding that antibodies and not T cells are the key mediators of immunity to borrelia infections (3, 17, 38, 40). Of the two serotypes tested, which are identical except in their variable major protein, we found that the spirochetal load and the loss of cardiomyocytes were significantly greater with *B. turicatae* serotype 2. This is consistent with previous findings that serotype 2 causes more severe systemic disease. Cardiomyocyte loss was more severe at the base and periphery of the heart, corresponding to areas of infiltration by activated macrophages and upregulation of the inflammatory cytokine IL-6. Significant apoptosis was observed in persistently infected hearts with induction of several caspases, most notably caspase-1 produced by activated macrophages.

In nonhuman primates inoculated with North American strains of *B. burgdorferi*, carditis was found in all the animals, including some examined more than 2 years after inoculation (11). Immunosuppression with steroids resulted in much higher spirochetal load in the heart and severe carditis (13). Carditis is also very common in immunocompetent and immunosuppressed rodents inoculated with *B. burgdorferi*. *scid* and NIH-3 mice develop pancarditis with infiltrations of mononuclear cells in the endocardium, myocardium, and pericardium, and spirochetes are readily seen in the myocardium (18, 51). The majority of Syrian hamsters and inbred mice inoculated with *B. burgdorferi* also develop cardiac infection which is persistent (4, 22). *B. burgdorferi* has been shown to have a predilection for collagenous tissues in the base of the heart (4, 8, 13, 44). There appears to be a difference in the frequency of carditis among *B. burgdorferi* strains (57). Comparatively little is known about carditis in relapsing fever. We showed that *scid* mice develop severe myocarditis as a result of persistent infection with *B. turicatae* (16), and Gebbia and colleagues showed that plasminogen facilitates infection of the heart (21).

Switching between serotypes provides relapsing fever borrelias with a strategy not only to avoid the host's antibody response but also to exploit different microenvironments (16). Our finding that *B. turicatae* serotype 2 infected the heart in higher numbers compared with *B. turicatae* serotype 1 provides

further evidence of this. It is unclear whether expression of Vsp2 in *B. turicatae* serotype 2 favors the entry, multiplication, and/or retention of Vsp2-expressing spirochetes in the heart. When the spirochetal load in the heart was studied as a percentage of spirochetes simultaneously present in blood, we found that serotype 1 was better than serotype 2 at entering the heart (H. Gelderblom and D. Cadavid, unpublished). Since the growth rates between *B. turicatae* serotypes 1 and 2 are similar at least in vitro (12), it is more likely that Vsp2 improves the retention of serotype 2 in the heart. One way this may occur could be via better binding to extracellular matrix components, as has been shown for decorin binding lipoproteins of *B. burgdorferi* (33). In fact, recombinant Vsp2, but not Vsp1, has been shown to bind to heparin and dermatan sulfate (36). Further support of this was the finding that the preferred niche of *B.turicatae* in the heart is, similar to *B. burgdorferi* (13), collagenous areas.

The positive correlation between spirochetal load and loss of cardiomyocytes suggests that the spirochetes or their products are responsible for the loss of cardiomyocytes. The concordance between the localization of spirochetes, activated macrophages, IL-6, and caspase-1 and the areas where cardiomyocytes were lost points to a complex chain of events that begins with the infection, triggers inflammation, and ends with the loss of cardiomyocytes. Through their ability to induce production of cytokines by macrophages and to activate endothelium and other host cells, borrelia lipoproteins are likely responsible for the inflammatory response to the infection (48). Toll-like receptors (TLRs) are recently described transmembrane proteins with key roles in the induction of immune and inflammatory responses (1). Recently, the ability of eukaryotic cells to respond to borrelia lipoproteins was correlated with expression of Toll-like receptors 1 and 2 (26, 34). TLRs induce signal transduction pathways that lead to the activation of transcription factors of the NF-κB family, which in turn increase expression of several inflammatory mediators. Recent studies indicate that TLR2 can signal not only inflammation but also apoptosis, through MyD88 via Fas-associated death domain protein and caspase-8 (2). TLR2 can also activate caspase-1, resulting in proteolysis and secretion of mature IL-1β and IL-18 (2). TLR2 may be the link between borrelia infection and downstream events leading to loss of cardiomyocytes, including inflammation and apoptosis. However, the specific mechanism of cardiomyocyte apoptosis was not determined in the present study. Others have shown that borrelias induce

apoptosis on lymphocytes, which appears to be related to release of cytokines (30, 47). Persistent expression of relapsing fever Vsp's in the heart may be responsible for the loss of cardiomyocytes. In vitro others have shown that OspA of *B. burgdorferi* can cause apoptosis of rhesus astrocytes (50). One way this may occur is by stimulation of the TLR2-MyD88 signaling pathway with secondary activation of Fas-associated domain protein and caspase-8 (2).

Caspase-1 and caspase-11 had been traditionally considered to have importance in inflammation but not in apoptosis. Murine caspases 1 and 11 (the latter is the murine homologue of human caspases 4 and 5) are crucial for propagation of acute inflammatory responses that rely on IL-1β and other cytokines (29, 31). Caspase-1-deficient mice had a major defect in the production of mature IL-1β and impaired IL-1α synthesis and diminished secretion of tumor necrosis factor and IL-6 in response to lipopolysaccharide stimulation (32). Macrophages from caspase-1-deficient mice are defective in LPS-induced gamma interferon production (19) and are highly resistant to the lethal effects of endotoxin (32). Caspase-1 may promote apoptosis by modulating the apoptotic cascade and/or by activating the immune system. The overexpression of caspase-1 causes fibroblasts to undergo apoptosis (20, 39). It has been proposed that caspase-1 activation may increase the cleavage of substrates that either mediate cell death or are required for cell survival (20). One such molecule may be tumor necrosis factor α (10, 50). A recent study found that caspase-1 acts in synergy with hypoxia to stimulate caspase-3-mediated apoptosis (53).

Our results revealed that, in contrast to immunocompetent mice that were resistant to relapsing fever carditis, antibody-deficient mice develop persistent borrelia infection of the heart with significant loss of cardiomyocytes and prominent apoptosis. Another novel finding is the prominent upregulation of caspase-1. Future studies may elucidate the mechanism by which borrelias or their products cause apoptosis of cardiomyocytes and the role of caspase-1 in this process.

ACKNOWLEDGMENTS

REFERENCES

1. **Akira, S.** 2000. Toll-like receptors: lessons from knockout mice. Biochem. Soc. Trans. **28:**551–556.
2. **Aliprantis, A. O., R. B. Yang, D. S. Weiss, P. Godowski, and A. Zychlinsky.** 2000. The apoptotic signaling pathway activated by Toll-like receptor-2. EMBO J. **19:**3325–3336.
3. **Alugupalli, K. R., R. M. Gerstein, J. Chen, E. Szomolanyi-Tsuda, R. T. Woodland, and J. M. Leong.** 2003. The resolution of relapsing fever borreliosis requires IgM and is concurrent with expansion of B1b lymphocytes. J. Immunol. **170:**3819–3827.
4. **Armstrong, A. L., S. W. Barthold, D. H. Persing, and D. S. Beck.** 1992. Carditis in Lyme disease susceptible and resistant strains of laboratory mice infected with Borrelia burgdorferi. Am. J. Trop. Med. Hyg. **47:**249–258.
5. **Asch, E. S., D. I. Bujak, M. Weiss, M. G. Peterson, and A. Weinstein.** 1994. Lyme disease: an infectious and postinfectious syndrome. J. Rheumatol. **21:**454–461.
6. **Bai, Y., K. Narayan, D. Dail, M. Sondey, E. Hodzic, S. W. Barthold, A. R. Pachner, and D. Cadavid.** 2004. Spinal cord involvement in the nonhuman primate model of Lyme disease. Lab. Investig. **84:**160–172.
7. **Barbour, A.** 1984. Isolation and cultivation of Lyme disease spirochetes. Yale J. Biol. Med. **57:**521–525.
8. **Barthold, S. W., D. H. Persing, A. L. Armstrong, and R. A. Peeples.** 1991. Kinetics of Borrelia burgdorferi dissemination and evolution of disease after intradermal inoculation of mice. Am. J. Pathol. **139:**263–273.
9. **Bartunek, P., V. Mrazek, K. Gorican, R. Bina, S. Listvanova, and J. Zapletalova.** 2001. Borrelia infection as a cause of carditis (a long-term study). Wien Klin. Wochenschr. **113:**38–44.
10. **Bogdan, I., S. L. Leib, M. Bergeron, L. Chow, and M. G. Tauber.** 1997. Tumor necrosis factor-alpha contributes to apoptosis in hippocampal neurons during experimental group B streptococcal meningitis. J. Infect. Dis. **176:**693–697.
11. **Cadavid, D., Y. Bai, E. Hodzic, K. Narayan, S. W. Barthold, and A. R. Pachner.** 2004. Cardiac involvement in non-human primates infected with the Lyme disease spirochete Borrelia burgdorferi. Lab. Investig. **84:**1439–1450.
12. **Cadavid, D., V. Bundoc, and A. G. Barbour.** 1993. Experimental infection of the mouse brain by a relapsing fever Borrelia species: a molecular analysis. J. Infect. Dis. **168:**143–151.
13. **Cadavid, D., T. O'Neill, H. Schaefer, and A. R. Pachner.** 2000. Localization of Borrelia burgdorferi in the nervous system and other organs in a nonhuman primate model of lyme disease. Lab. Investig. **80:**1043–1054.
14. **Cadavid, D., A. R. Pachner, L. Estanislao, R. Patalapati, and A. G. Barbour.** 2001. Isogenic serotypes of *Borrelia turicatae* show different localization in the brain and skin of mice. Infect. Immun. **69:**3389–3397.
15. **Cadavid, D., P. M. Pennington, T. A. Kerentseva, S. Bergstrom, and A. G. Barbour.** 1997. Immunologic and genetic analyses of VmpA of a neurotropic strain of *Borrelia turicatae*. Infect. Immun. **65:**3352–3360.
16. **Cadavid, D., D. D. Thomas, R. Crawley, and A. G. Barbour.** 1994. Variability of a bacterial surface protein and disease expression in a possible mouse model of systemic Lyme borreliosis. J. Exp. Med. **179:**631–642.
17. **Connolly, S. E., and J. L. Benach.** 2001. Cutting edge: the spirochetemia of murine relapsing fever is cleared by complement-independent bactericidal antibodies. J. Immunol. **167:**3029–3032.
18. **Defosse, D. L., P. H. Duray, and R. C. Johnson.** 1992. The NIH-3 immunodeficient mouse is a model for Lyme borreliosis myositis and carditis. Am. J. Pathol. **141:**3–10.
19. **Fantuzzi, G., A. J. Puren, M. W. Harding, D. J. Livingston, and C. A. Dinarello.** 1998. Interleukin-18 regulation of interferon gamma production and cell proliferation as shown in interleukin-1beta-converting enzyme (caspase-1)-deficient mice. Blood **91:**2118–2125.
20. **Friedlander, R. M., V. Gagliardini, R. J. Rotello, and J. Yuan.** 1996. Functional role of interleukin 1 beta (IL-1 beta) in IL-1 beta-converting enzyme-mediated apoptosis. J. Exp. Med. **184:**717–724.
21. **Gebbia, J. A., J. C. Monco, J. L. Degen, T. H. Bugge, and J. L. Benach.** 1999. The plasminogen activation system enhances brain and heart invasion in murine relapsing fever borreliosis. J. Clin. Investig. **103:**81–87.
22. **Goodman, J. L., P. Jurkovich, C. Kodner, and R. C. Johnson.** 1991. Persistent cardiac and urinary tract infections with *Borrelia burgdorferi* in experimentally infected Syrian hamsters. J. Clin. Microbiol. **29:**894–896.
23. **Grollier, G., F. Galateau, P. Scanu, B. Valette, G. Bureau, J. P. Carpentier, G. Cloatre, and J. C. Potier.** 1992. Lyme's disease, a possible cause of isolated acute myocarditis. Presse Med. **21:**843–846.
24. **Hendricks, O., P. Kjaeldgaard, and I. Koldbaek.** 2003. Borrelia burgdorferi myocarditis. Ugeskr Laeger **165:**1570.
25. **Hinnebusch, B. J., A. G. Barbour, B. I. Restrepo, and T. G. Schwan.** 1998. Population structure of the relapsing fever spirochete *Borrelia hermsii* as indicated by polymorphism of two multigene families that encode immunogenic outer surface lipoproteins. Infect. Immun. **66:**432–440.
26. **Hirschfeld, M., C. J. Kirschning, R. Schwandner, H. Wesche, J. H. Weis, R. M. Wooten, and J. J. Weis.** 1999. Cutting edge: inflammatory signaling by Borrelia burgdorferi lipoproteins is mediated by toll-like receptor 2. J. Immunol. **163:**2382–2386.
27. **Kang, S. J., S. Wang, H. Hara, E. P. Peterson, S. Namura, S. Amin-Hanjani, Z. Huang, A. Srinivasan, K. J. Tomaselli, N. A. Thornberry, M. A. Moskowitz, and J. Yuan.** 2000. Dual role of caspase-11 in mediating activation of caspase-1 and caspase-3 under pathological conditions. J. Cell Biol. **149:**613–622.
28. **Kozakiewicz, H., and B. Neuman-Tomaszewska.** 1980. Case of coxsackie virus infection with multiple organ involvement. Wiad Lek. **33:**293–295.
29. **Kuida, K., J. A. Lippke, G. Ku, M. W. Harding, D. J. Livingston, M. S. Su, and R. A. Flavell.** 1995. Altered cytokine export and apoptosis in mice deficient in interleukin-1 beta converting enzyme. Science **267:**2000–2003.
30. **Leung, W. K., Q. Wu, P. M. Hannam, B. C. McBride, and V. J. Uitto.** 2002. Treponema denticola may stimulate both epithelial proliferation and apoptosis through MAP kinase signal pathways. J. Periodont. Res. **37:**445–455.
31. **Li, P., H. Allen, S. Banerjee, S. Franklin, L. Herzog, C. Johnston, J. McDowell, M. Paskind, L. Rodman, J. Salfeld, et al.** 1995. Mice deficient in IL-1 beta-converting enzyme are defective in production of mature IL-1 beta and resistant to endotoxic shock. Cell **80:**401–411.
32. **Li, P., H. Allen, S. Banerjee, and T. Seshadri.** 1997. Characterization of mice deficient in interleukin-1 beta converting enzyme. J. Cell Biochem. **64:**27–32.
33. **Liang, F. T., E. L. Brown, T. Wang, R. V. Iozzo, and E. Fikrig.** 2004. Protective niche for Borrelia burgdorferi to evade humoral immunity. Am. J. Pathol. **165:**977–985.

34. **Lien, E., T. J. Sellati, A. Yoshimura, T. H. Flo, G. Rawadi, R. W. Finberg, J. D. Carroll, T. Espevik, R. R. Ingalls, J. D. Radolf, and D. T. Golenbock.** 1999. Toll-like receptor 2 functions as a pattern recognition receptor for diverse bacterial products. J. Biol. Chem. **274:**33419–33425.

35. **Luger, A., F. Gschnait, and G. Niebauer.** 1987. Economic aspects of serologic syphilis tests in routine screening in Viennese hospital facilities. Wien Klin Wochenschr. **99:**808–811.

36. **Magoun, L., W. R. Zuckert, D. Robbins, N. Parveen, K. R. Alugupalli, T. G. Schwan, A. G. Barbour, and J. M. Leong.** 2000. Variable small protein (Vsp)-dependent and Vsp-independent pathways for glycosaminoglycan recognition by relapsing fever spirochaetes. Mol. Microbiol. **36:**886–897.

37. **McCue, M. J., and E. E. Moore.** 1979. Myocarditis with microabscess formation caused by Listeria monocytogenes associated with myocardial infarct. Hum. Pathol. **10:**469–472.

38. **McKisic, M. D., and S. W. Barthold.** 2000. T-cell-independent responses to *Borrelia burgdorferi* are critical for protective immunity and resolution of Lyme disease. Infect. Immun. **68:**5190–5197.

39. **Miura, M., H. Zhu, R. Rotello, E. A. Hartwieg, and J. Yuan.** 1993. Induction of apoptosis in fibroblasts by IL-1 beta-converting enzyme, a mammalian homolog of the C. elegans cell death gene ced-3. Cell **75:**653–660.

40. **Newman, K., Jr., and R. C. Johnson.** 1984. T-cell-independent elimination of *Borrelia turicatae*. Infect. Immun. **45:**572–576.

41. **Nosanchuk, J. D.** 2002. Fungal myocarditis. Front. Biosci. **7:**d1423–d1438.

42. **Oltvai, Z. N., C. L. Milliman, and S. J. Korsmeyer.** 1993. Bcl-2 heterodimerizes in vivo with a conserved homolog, Bax, that accelerates programmed cell death. Cell **74:**609–619.

43. **Orloski, K. A., E. B. Hayes, G. L. Campbell, and D. T. Dennis.** 2000. Surveillance for Lyme disease–United States, 1992–1998. Morb. Mortal. Wkly. Rep. CDC Surveil. Summ. **49:**1–11.

44. **Pachner, A. R., J. Basta, E. Delaney, and D. Hulinska.** 1995. Localization of Borrelia burgdorferi in murine Lyme borreliosis by electron microscopy. Am. J. Trop. Med. Hyg. **52:**128–133.

45. **Penninger, J. M., and K. Bachmaier.** 2000. Review of microbial infections and the immune response to cardiac antigens. J. Infect. Dis. **181**(Suppl. 3)**:** S498–S504.

46. **Pennington, P. M., D. Cadavid, and A. G. Barbour.** 1999. Characterization of VspB of *Borrelia turicatae*, a major outer membrane protein expressed in blood and tissues of mice. Infect. Immun. **67:**4637–4645.

47. **Perticarari, S., G. Presani, M. Prodan, M. Granzotto, R. Murgia, and M. Cinco.** 2003. Lymphocyte apoptosis co-cultured with Borrelia burgdorferi. Microb. Pathog. **35:**139–145.

48. **Radolf, J. D., L. L. Arndt, D. R. Akins, L. L. Curetty, M. E. Levi, Y. Shen, L. S. Davis, and M. V. Norgard.** 1995. Treponema pallidum and Borrelia burgdorferi lipoproteins and synthetic lipopeptides activate monocytes/macrophages. J. Immunol. **154:**2866–2877.

49. **Radolf, J. D., M. S. Goldberg, K. Bourell, S. I. Baker, J. D. Jones, and M. V. Norgard.** 1995. Characterization of outer membranes isolated from *Borrelia burgdorferi*, the Lyme disease spirochete. Infect. Immun. **63:**2154–2163.

50. **Ramesh, G., A. L. Alvarez, E. D. Roberts, V. A. Dennis, B. L. Lasater, X. Alvarez, and M. T. Philipp.** 2003. Pathogenesis of Lyme neuroborreliosis: Borrelia burgdorferi lipoproteins induce both proliferation and apoptosis in rhesus monkey astrocytes. Eur. J. Immunol. **33:**2539–2550.

51. **Schaible, U. E., S. Gay, C. Museteanu, M. D. Kramer, G. Zimmer, K. Eichmann, U. Museteanu, and M. M. Simon.** 1990. Lyme borreliosis in the severe combined immunodeficiency (scid) mouse manifests predominantly in the joints, heart, and liver. Am. J. Pathol. **137:**811–820.

52. **Stanek, G., J. Klein, R. Bittner, and D. Glogar.** 1990. Isolation of Borrelia burgdorferi from the myocardium of a patient with longstanding cardiomyopathy. N. Engl. J. Med. **322:**249–252.

53. **Syed, F. M., H. S. Hahn, A. Odley, Y. Guo, J. G. Vallejo, R. A. Lynch, D. L. Mann, R. Bolli, and G. W. Dorn, 2nd.** 2005. Proapoptotic effects of caspase-1/interleukin-converting enzyme dominate in myocardial ischemia. Circ. Res. **96:**1103–1109.

54. **van der Linde, M. R., H. J. Crijns, J. de Koning, J. A. Hoogkamp-Korstanje, J. J. de Graaf, D. A. Piers, A. van der Galien, and K. I. Lie.** 1990. Range of atrioventricular conduction disturbances in Lyme borreliosis: a report of four cases and review of other published reports. Br. Heart J. **63:**162–168.

55. **Vasiljevic, Z., R. Dmitrovic, Z. Naumovic, M. Ostojic, M. Radosavljevic, A. Karadzic, M. Prostran, and M. Colic.** 1996. Common form of Lyme borreliosis carditis–complete heart block with syncope: report on 3 cases. Cardiology **87:**76–78.

56. **Woolf, P. K., E. M. Lorsung, K. S. Edwards, K. I. Li, S. J. Kanengiser, R. M. Ruddy, and M. H. Gewitz.** 1991. Electrocardiographic findings in children with Lyme disease. Pediatr. Emerg. Care. **7:**334–336.

57. **Zeidner, N. S., B. S. Schneider, M. C. Dolan, and J. Piesman.** 2001. An analysis of spirochete load, strain, and pathology in a model of tick-transmitted Lyme borreliosis. Vector Borne Zoonotic Dis. **1:**35–44.